Source-receiver migration of multiple reflections

Guojian Shan, Stanford University*

SUMMARY

Multiple reflections are usually considered as noise and many methods are developed to attenuate them. However, similarly to primary reflections, multiple reflections are created by subsurface reflectors and contain the reflectivity information. We can image multiples, regarding the primaries as the source. Traditional source-receiver migration assumes that the source is impulse function. I generalize the source-receiver migration to an arbitrary source, and apply it to the migration of multiple reflections. A complex synthetic data is used to test the theory. Results show that my multiple migration algorithm is effective for imaging the multiple contaminated data.

INTRODUCTION

Multiple reflections are traditionally regarded as noise and attenuated (Verschuur and Berkhout, 1997; Guitton et al., 2001). However, some works have treated multiple reflections as signal and tried to image them. Reiter et al. (1991) image deep-water multiples applying Kirchoff scheme. Sheng (2001) migrated multiples in CDP data applying crosscorrelogram migration. Berkhout and Verschuur (1994) and Guitton (2002) image the multiples with shot-profile migration. Brown (2002) jointly image the primaries and multiples with least-square methods. In this paper, I present source-receiver migration for multiples. I calculate pseudo-primary gather by cross-correlating primary with multiple at the surface, and run a traditional source-receiver migration algorithm without any change on the pseudo-primary data to get the image.

Biondi (2002) derived the equivalence between shot-profile migration and source-receiver migration, given the assumption that the source is an impulse function, the image condition is cross-correlation, and one-wave downward continuation method is used for wavefield propagation. Shan and Zhang (2003) generalized the traditional source-receiver migration for arbitrary source, and demonstrated the equivalence between shot-profile migration and source-receiver migration. As a special case of generalized source-receiver migration, multiple migration has a complicated source–the primary reflection wavefield, so multiple migration is a good numerical test for the equivalence between shot-profile migration and source-receiver migration.

In this paper, I review the theory of the generalized source-receiver migration and give the algorithm to create pseudo-primary data for multiple migration. I present poststack and prestack multiple migration of a 2-D synthetic data, and compare the migration result with the migration of original data.

THEORY

Traditional source-receiver migration assumes that the source is an impulse function and the migration is based on the survey sinking. Source-receiver migration downward continues the CMP gather $P(x,h,z,\omega)$ into the subsurface by the Double Square Root equation

$$\frac{\partial}{\partial z}P = \left(\frac{i\omega}{v_s}\sqrt{1+\frac{v_s^2}{\omega^2}\frac{\partial^2}{\partial x_s^2}} + \frac{i\omega}{v_r}\sqrt{1+\frac{v_r^2}{\omega^2}\frac{\partial^2}{\partial x_r^2}} \right) P, \qquad (1)$$

where x is midpoint, h is half offset, x_s is the source point, x_r is the receiver point, $v_s = v(x_s,z)$ and $v_r = v(x_r,z)$. It images by extracting the wavefield at zero subsurface offset $P(x,h=0,z,\omega)$ and adding along all frequencies. In the generalized source-receiver migration, instead of using CMP gather of the recorded data directly, cross-correlation between source $D(x_D,z=0,\omega,s)$ and receiver $U(x_U,z=0,\omega,s)$ wavefields at surface are extrapolated into the media. Namely, the wavefield to be downward continued by the Double Square Root equation is

$$P(x,h,z=0,\omega) = \sum_s U(x_U,z=0,\omega,s)\bar{D}(x_D,z=0,\omega,s) \qquad (2)$$

where $x=(x_U+x_D)/2$, $h=(x_U-x_D)/2$ and s means an areal shot. When the source is an impulse function, the cross-correlation between source and receiver wavefields is exactly the CMP gather of recorded data and the generalized source-receiver migration algorithm is exactly same as the traditional source-receiver migration.

Source-receiver migration of multiple reflections is a special case of generalized source-receiver migration, in which the source wavefield is the primary reflection and the receiver wavefield is the corresponding multiple reflection. The wavefield to be downward continued is the cross-correlation between primary+multiple and multiple. Since it behaves very similarly to a primary, I call it pseudo-primary data. There are two steps for source-receiver migration of multiples. First, pseudo-primary data are calculated by cross-correlating the primary+multiple with multiple reflections at the surface. Second, traditional source-receiver migration is run on the pseudo-primary data. Figure 1 illustrates the principle of source-receiver migration of multiples. The phase of the trace at (x,h) of pseudo-primary data is exactly same as a trace at (x,h) from CMP gather of primary, if we would have put a source at x_D and a receiver at x_U.

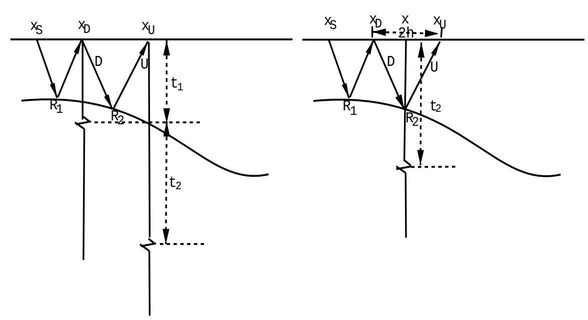

Figure 1: Left: Two traces in originally recorded data. The trace at x_D records the primary reflection travel time t_1 of $x_S \to R_1 \to x_D$. The trace at x_U records the multiple reflection travel time t_1+t_2 of $x_S \to R_1 \to X_D \to R_2 \to x_U$. Right: The trace of pseudo-primary data related to trace x_D and x_U. The trace at (x,h) is the cross-correlation between trace x_D and trace x_U, where x, h are mid-point and half offset of x_D and x_U respectively.

Zero-offset data is very important in amplitude work, but it is never recorded in real survey. we can get the zero-offset dataset from the pseudo-primary data very easily. In equation (2), let $x_U = x_D = x$, we can get the zero-offset surface dataset

$$P(x,h=0,z=0,\omega) = \sum_s U(x,z=0,\omega)\bar{D}(x,z=0,\omega). \qquad (3)$$

The zero-offset dataset from pseudo-primary data provide real information about z_0 reflectivity. Figure 2 illustrates the way to get zero-offset surface dataset of pseudo-primary data. The phase information of the zero-offset dataset of the pseudo-primary data is

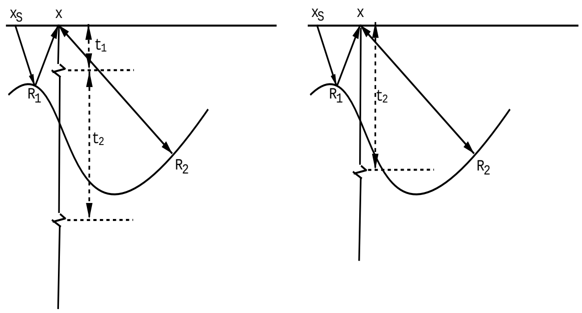

Figure 2: Left: One trace in originally recorded data. The trace at x has two impulse. The first one records the travel time of primary reflection t_1: $x_S \to R_1 \to x$ and the second one records the travel time of multiple reflection t_2: $x_S \to R_1 \to x \to R_2 \to x$. Right: Zero-offset dataset of pseudo-primary data. The trace in the pseudo-primary data is the cross-correlation of the trace in left figure with itself. The traveltime of impulse in the trace is double traveltime between x and R_2.

exactly same as the zero-offset gotten if we would have put a source and receiver at x.

SYNTHETIC DATA EXAMPLE

In this section, I test my theory of multiple migration on a modified version of the 2.5-D Amoco dataset (Etgen and Regone, 1998; Dellinger et al., 2000), which was also used for shot-profile migration of multiple reflections (Guitton, 2002).

Figure 3 shows the velocity model of the Amoco dataset. In the survey, a 500 meters water layer is added and 32 shots are computed with a split-spread geometry (Guitton, 2002).

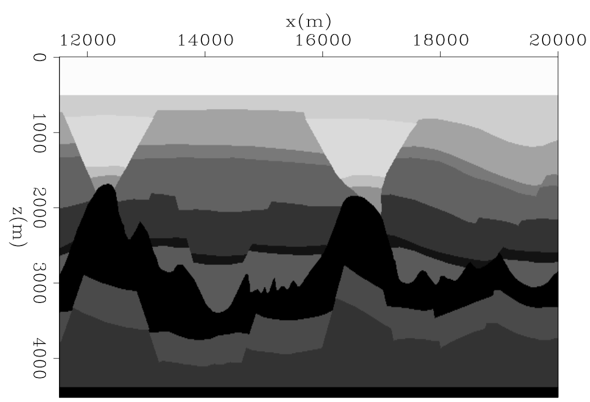

Figure 3: The velocity model for the synthetic data.

Pseudo-primary for multiple migration

Figure 1 and Figure 2 show the algorithm to create the pseudo-primary data for multiple migration. I cross-correlate the primary+ multiple with multiple at surface and extract the zero-offset dataset and one shot dataset for comparison.

Figure 4 shows the zero-offset dataset from both originally recorded dataset and pseudo-primary dataset.the zero-offset dataset is very coarse, since only 32 shots are recorded in the original dataset, while the zero-offset dataset from pseudo-primary data is continuous, since every trace in the originally recorded data can be a areal shot in pseudo-primary data. Nevertheless, as shown in Figure 2, the zero-offset dataset from pseudo-primary data is very similar to the originally recorded data.

Figure 5 displays the comparison between one shot from originally recorded data and from pseudo-primary data. Although the pseudo-primary shot is pretty noisy, it has similar structure to the shot from the original data.

Migration for zero-offset multiple reflections

It is interesting that cross-correlation between primary reflection and multiple reflection can provide real zero-offset dataset, which can be processed by poststack migration. Figure 6 display the post-stack migration of the zero-offset dataset of pseudo-primary data. The migration result is pretty noisy because only one offset data is used while usually all offsets data are stacked after NMO in post-stack migration. But we can still dig out the subsurface structure from the image. We can get the top and bottom of the salt, and the flat line below the salt.

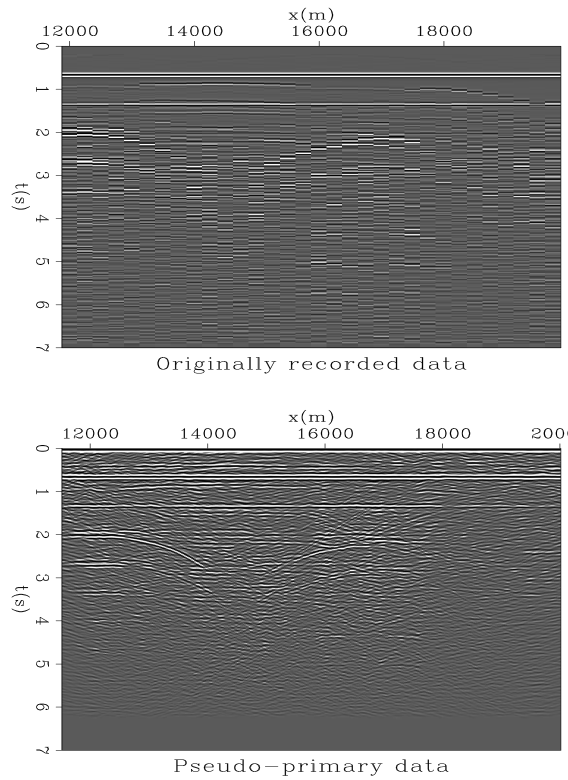

Figure 4: Zero offset dataset. Above: The zero offset dataset of originally recorded data. Below: The zero offset dataset of pseudo-primary data.

Source-receiver migration for multiple reflections

For comparison, I migrate the primaries with Fourier finite difference for the Double Square Root equation (Zhang and Shan, 2001), and the migration result is presented in Figure 7. There are a lot of hyperbolas because the shots recorded are very sparse. I migrate the multiple reflection using both split-step method for the Double Square Root equation (Popovici, 1996) and Fourier finite difference for the Double Square Root equation, in which the average velocity is used for reference velocity. The migration results are present in Figure 8 and Figure 9. The migration result of multiple (Figure 8,9)is similar to primary(Figure 7), although the migration of primary is sharper and less noisy.

It is not easy to separate the multiple from original data in prac-

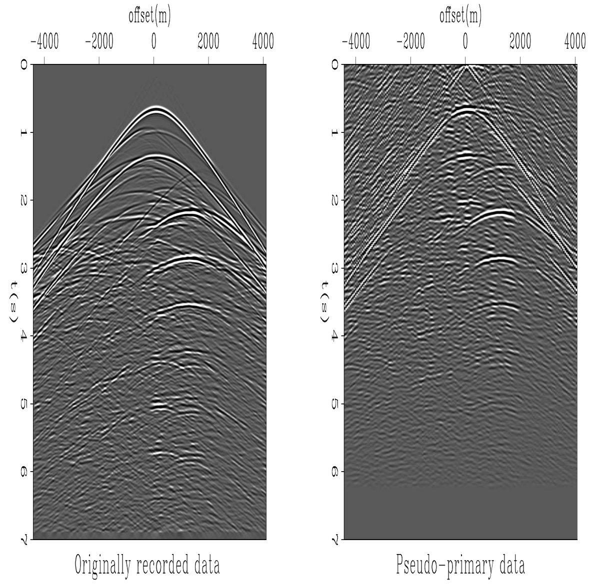

Figure 5: One shot dataset at 16000m. Left: One shot dataset of primary with multiples. Right: One shot dataset of pseudo-primary data.

tice. And the separation costs a lot of computation time. Instead of cross-correlating the primary+multiple with multiple, I cross-correlate the whole recorded data (primary+multiple) with itself and then run source-receiver migration. Figure 10 presents the migration result. The cross-correlation between primary reflection and primary reflection does add some noise to the image. We can see the fake reflector, which is mainly caused by the cross-correlation between water bottom reflection and the reflection below water bottom in primary. Nevertheless, the image is interpretable.

The amplitude of primary reflection at different location and different time are different. So the multiple reflection have different amplitude source. It is important to do amplitude balance for the pseudo-primary data before migration. I apply deconvolution (Claerbout, 1999) instead of cross-correlation at the surface data, namely the pseudo-primary data for source-receiver migration are calculated by

$$P(x,h,z=0,\omega) = \sum_s \frac{U(x_U,z=0,\omega,s)\bar{D}(x_D,z=0,\omega,s)}{D(x_D,z=0,\omega,s)\bar{D}(x_D,z=0,\omega,s)+\epsilon^2}. \quad (4)$$

Figure 11 show the migration result while deconvolution is used for creating pseudo-primary data. Besides the amplitude balancing, it also has better resolution.

CONCLUSIONS

I have shown the theory of source-receiver migration for multiple reflections, regarding the primaries as source. The 2-D complex synthetic data test prove that multiples can be correctly imaged with the generalized source-receiver migration method and provide structural information of the subsurface.

ACKNOWLEDGMENTS

I would like to thank Amoco for making the synthetic velocity available and the sponsors of Stanford Exploration Project for their financial support. I would like also to thank Antoine Guitton and Morgan Brown for many useful discussions.

REFERENCES

Berkhout, A. J., and Verschuur, D. J., 1994, Multiple technology: Part 2, migration of multiple reflections: 64th Ann. Internat. Mtg, Soc. Expl. Geophys., Expanded Abstracts, 1497–1500.

Biondi, B., 2002, Equivalence of source-receiver migration and shot-profile migration: Geophysics, accepted for publication.

Brown, M., 2002, Least-squares joint imaging of primaries and multiples: 72st Ann. Internat. Mtg., Soc. Expl. Geophys., Expanded Abstracts, 890–893.

Claerbout, J., 1999, Geophysical estimation by example: Environmental soundings image enhancement: Stanford Exploration Project, `http://sepwww.stanford.edu/sep/prof/`.

Dellinger, J. A., Gray, S. H., Murphy, G. E., and Etgen, J. T., 2000, Efficient 2.5-D true-amplitude migration: Geophysics, **65**, no. 03, 943–950.

Etgen, J., and Regone, C., 1998, Strike shooting, dip shooting, widepatch shooting - Does prestack depth migration care? A model study.: 68th Ann. Internat. Mtg, Soc. Expl. Geophys., Expanded Abstracts, 66–69.

Guitton, A., Brown, M., Rickett, J., and Clapp, R., 2001, Multiple attenuation using a t-x pattern-based subtraction method: 71st Ann. Internat. Mtg, Soc. Expl. Geophys., Expanded Abstracts, 1305–1308.

Guitton, A., 2002, Shot-profile migration of mutiple reflections: 72st Ann. Internat. Mtg., Soc. Expl. Geophys., Expanded Abstracts, 1296–1299.

Popovici, A. M., 1996, Prestack migration by split-step DSR: Geophysics, **61**, no. 05, 1412–1416.

Reiter, E. C., Toksoz, M. N., Keho, T. H., and Purdy, G. M., 1991, Imaging with deep-water multiples: Geophysics, **56**, no. 07, 1081–1086.

Shan, G., and Zhang, G., 2003, Equivalence between shot-profile and source-receiver migration: Equivalence between shot-profile and source-receiver migration:.

Sheng, J., 2001, Migration multiples and primaries in CDP data by crosscorrelogram migration: 71st Ann. Internat. Mtg, Soc. Expl. Geophys., Expanded Abstracts, 1297–1300.

Verschuur, D. J., and Berkhout, A. J., 1997, Estimation of multiple scattering by iterative inversion, Part II: Practical aspects and examples: Geophysics, **62**, no. 05, 1596–1611.

Zhang, G., and Shan, G., 2001, Helical scheme for 2-D prestack migration based on double-square-root equation: 71st Ann. Internat. Mtg, Soc. Expl. Geophys., Expanded Abstracts, 1057–1060.

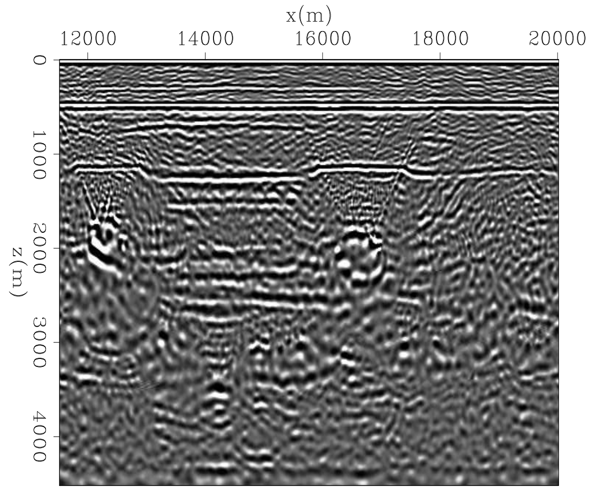

Figure 6: Poststack migration of zero_offset dataset.

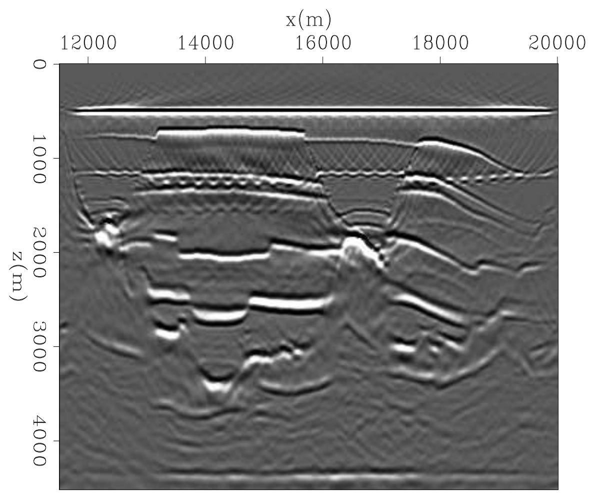

Figure 7: Migration result of originally recorded data.

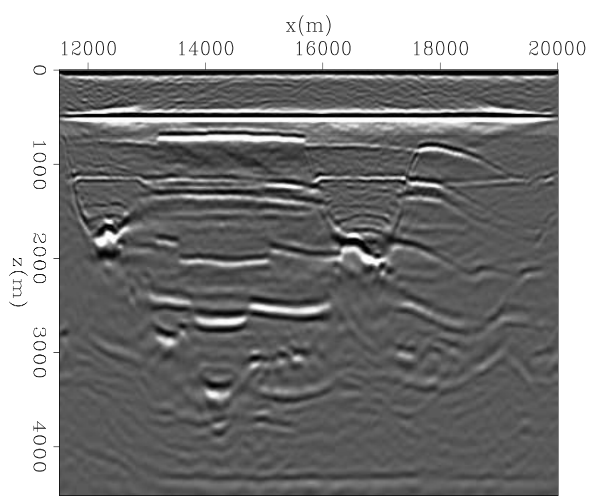

Figure 8: Imaging of multiples by split-step of DSR.

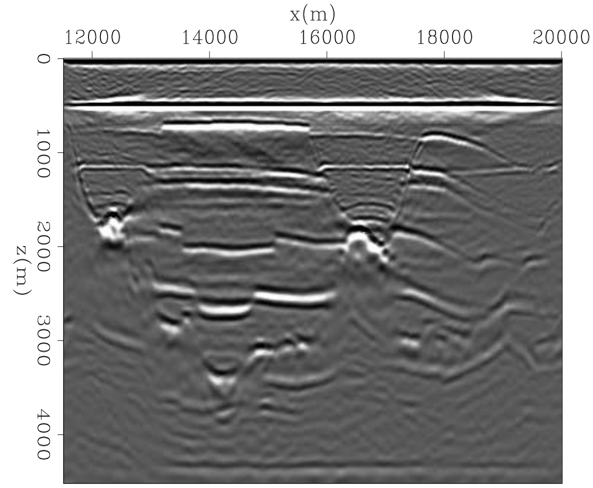

Figure 9: Imaging of multiples by FFD of DSR.

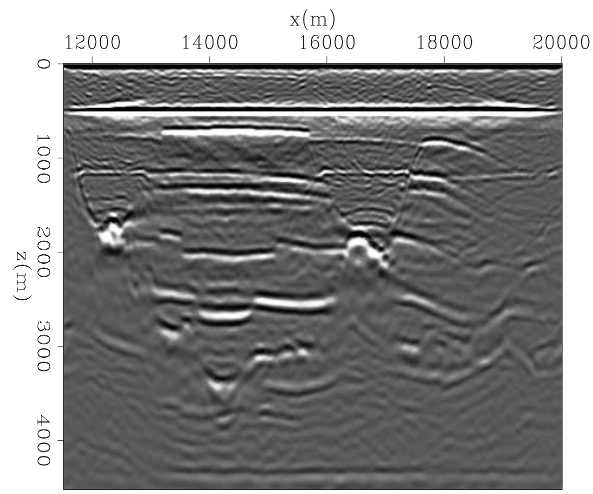

Figure 10: Migration of cross-correlation between primary+multiple and primary+multiple.

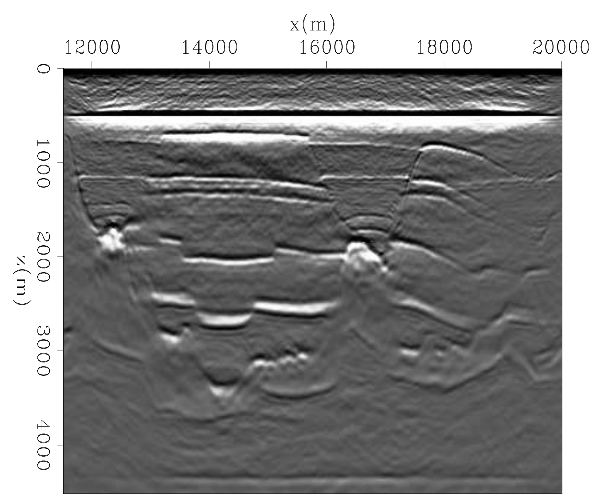

Figure 11: Imaging of multiples after amplitude balance.